

FATIGUE-INDUCED FRACTURE OF PERVIOUS CONCRETE: PHYSICAL AND NUMERICAL EXPERIMENTATION

SONOKO ICHIMARU*, ALESSANDRO FASCETTI †,
AND JOHN E. BOLANDER‡

*University of California, Davis
Davis, CA USA
e-mail: sichimaru@ucdavis.edu

†Sapienza Università di Roma
Roma, Italy
e-mail: alessandro.fascetti@uniroma1.it

‡University of California, Davis
Davis, CA USA
e-mail: jebolander@ucdavis.edu

Key words: Pervious concrete, Fatigue, Microcracking, Image Analysis

Abstract. Two types of pervious concrete are used to form small-scale specimens, which are subjected to fatigue loading. The first type is produced with a gap-grading of natural aggregates; the second type is produced with monosized spherical aggregates. Loading is applied via constant amplitude displacement cycles and reduction in specimen compliance is monitored. Loading is stopped at various stages prior to specimen failure to enable the investigation of damage progression using dye impregnation techniques. The second type of pervious concrete, based on spherical aggregates, lends itself to computer modeling. With respect to the aggregate positions, a one-to-one correspondence is sought between the experimental and numerical models. With further developments, this combined use of physical and numerical experimentation will provide insight into the roles of paste distribution and the interface phase on pervious concrete performance under fatigue loading.

1 Introduction

Pervious concretes offers several desirable properties, most notably high hydraulic conductivity. The large, connected pore structure is advantageous in applications where drainage and ground water recharge are sought. Recent applications are not only limited to pavement systems but also extend to other environmentally conscious projects. For example, the macro-porous structure offers ample space for plant roots to inhabit the concrete interior. Related practices toward

green construction and conservation ecology are found in Japan [1].

Figure 1 schematically illustrates the composition of pervious concrete for the idealized case of mono-sized circular aggregates. In actual materials, a similar structure is obtained through the gap-grading of natural aggregates that are coated by cement paste. Large connected air voids can be obtained by controlling the aggregate size and paste content [2]. As porosity is increased, however, load transfer through the material in-

creasingly relies on the small paste bridges between neighboring aggregates. Stress concentrations in these bridges are thought to govern the fatigue resistance of pervious concrete. Damage development under cyclic loading is qualitatively different from what occurs during fatigue failure of ordinary concrete.

Herein, two types of pervious concrete specimens are produced by: 1) gap-grading of natural aggregates; and 2) use of mono-sized spherical aggregates. Those made with natural aggregate are subjected to three-point bending, whereas those made with spherical aggregates are subjected to cyclic loading in compression. The use of spherical aggregates facilitates the planned computational modeling of these experiments. Crack development is studied using dye penetration techniques.

As expected, fatigue resistance is affected by the bond properties of the aggregate-matrix interface. Similar to observations of ordinary concrete, fatigue behavior appears to be separated into different regimes: damage accumulates rapidly in the early loading cycles, followed by stable, progressive damage development prior to failure.

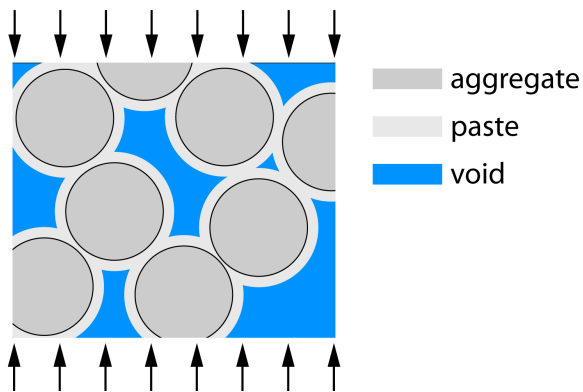


Figure 1: Schematic illustration of pervious concrete under load

2 Load testing and fracture characterization

Flexural and compressive load tests were conducted on specimens made with natural

aggregate and spherical glass aggregates, respectively. Testing was conducted in two stages. The first stage involved strength testing under monotonically increasing load. The second stage involved cyclic loading to a prescribed fraction of the strengths measured in the first stage. Within both stages, the ability to produce significant results was limited by the variability of the materials and the small number of specimens studied. Only basic observations are given here.

2.1 Three-point bend tests

Prismatic specimens of pervious concrete (with cross-section dimensions of 100×100 mm²) were produced for three-point bending tests. The mixture composition and proportions are given in Table 1. Natural coarse aggregate was used, along with a matrix composed of ordinary portland cement paste. The water-cement ratio is based on saturated surface-dry condition of the aggregates. Cast specimens were demolded after one day and then cured in lime saturated water until testing.

Table 1: Mixture composition and proportions for flexural test specimens (units: %wt)

water	cement	aggregate	SP*	VMA**
3.68	12.7	83.5	0.0060	0.076

* super-plasticizer

**viscosity modifying admixture

For several specimens, cyclic loading was halted prior to failure, so that internal cracking could be mapped using a dye penetration technique. More specifically, the mid-span portion of a damaged specimen was vacuum impregnated with low-viscosity epoxy resin mixed with fluorescent dye. Exposing cross-sections to UV light illuminated the pore structure and fine crack features.

Under three-point bending, fracture occurred by a single macro-crack that crossed the aggregate-paste bridges. The bridges

failed either by fracture of the matrix or by debonding at the matrix-aggregate interface, as shown in Figs. 2 and 3. There was no evidence of distributed micro cracking off the macro-crack plane. Furthermore, distributions of the material phases and porosity within the cross-section differ greatly from those of the idealized model shown in Fig. 1. In particular, the matrix phase is non uniformly distributed about the irregular aggregate sections.

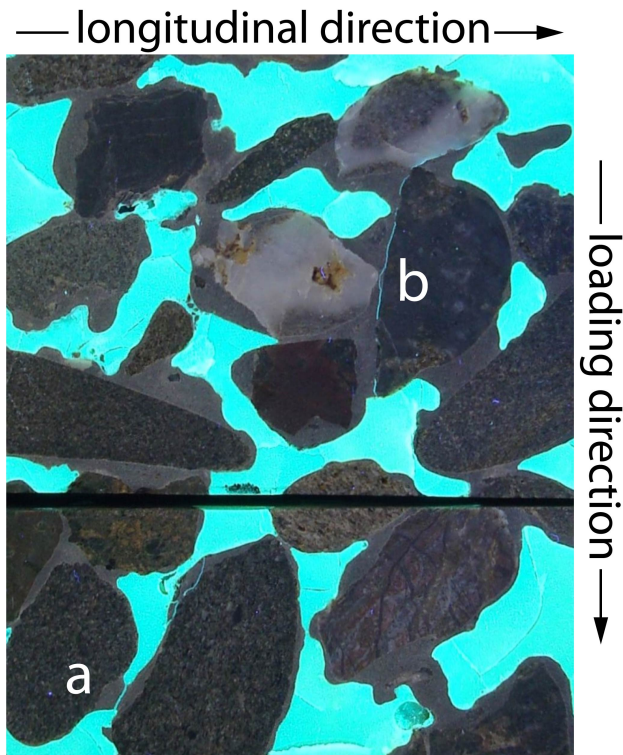


Figure 2: Porosity and crack identification on a material cross-section: a) matrix fracture; and b) fracture along aggregate-matrix interface.



Figure 3: Enlarged view of epoxy impregnated cracks within the matrix phase (left) and along the matrix-aggregate interface (right)

2.2 Compressive load tests

Specimen production

Cylindrical specimens of pervious concrete were produced using soda lime glass spheres (with nominal diameter $d_a = 10$ mm) as aggregates. The binder proportions, given in Table 2, were determined through a series of trials that sought uniform thickness of the paste coating the aggregates. Assessments of coating were based on visual appearance in the fresh state.

As received, the glass aggregates had smooth surfaces. In anticipation of poor bonding between those surfaces and the paste matrix, a fraction of the aggregates were tumbled in a drum containing water and silicon carbide particles. Such roughening of the surfaces also appeared to improve adherence of the fresh paste to the aggregate surfaces during mixing and specimen production.

Table 2: Mixture composition and proportions for compression test specimens (units: %wt)

water	cement	aggregate	SP*	VMA**
5.73	19.7	74.3	0.090	0.118

* super-plasticizer

**viscosity modifying admixture

Mixing of the cement paste was done in a 5-qt. Hobart mixer. The aggregates were manually introduced after mixing due to the small clearance between the mixer blades and container. The paste-aggregate mixture was introduced into 102 mm x 51 mm cylindrical molds. Upon filling each mold, the material was consolidated by applying a pressure of 33 kPa in the axial direction. Eight cylinder specimens were produced: two for image analyses of material structure; three for compressive strength testing; and three for fatigue testing. After one day, the specimens were removed from the molds and cured in lime saturated water until the time of test-

ing. For all load tests, the cylinder ends were capped with sulphur compound.



Figure 4: Effect of aggregate surface roughness on post-failure appearance: (a) unroughened surfaces; (b) roughened surfaces

Effects of aggregate surface roughness

Typical post-failure appearances of the aggregate-matrix interface, for either monotonic or cyclic loading, are shown in Fig. 4.

The glossy appearance of the matrix is an indication of low bond strength along the smooth aggregate surfaces. The appearance of specimens formed with roughened aggregates is qualitatively different and suggests improved bond properties. As seen in Fig. 4b, aggregate fracture occurs in some locations.

Fatigue loading results

Instead of counting the number of cycles to failure under force control, fatigue loading was done under displacement control. The amplitude of the displacement cycle, Δ , was based on the previous measurements of the compressive strength and axial stiffness of the specimen. Load was slowly increased up to the set point, which corresponds to $\delta = 0$ in Fig. 5a.

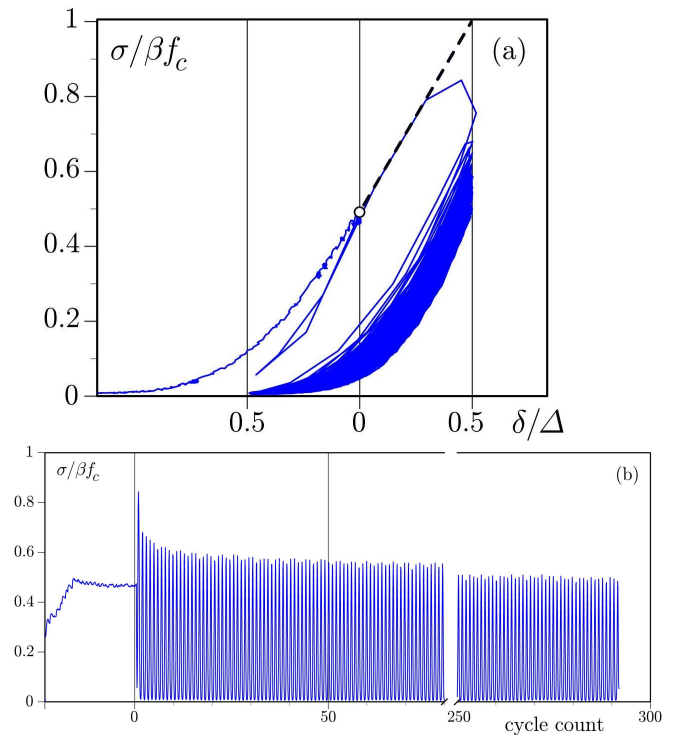


Figure 5: Typical fatigue test results: a) load versus controlled displacement; b) load versus cycle count

Cyclic loading commences from the set point with a half-amplitude of $\Delta/2$. Specimen compliance, which is a measure of damage development, increases with cycle count.

This specimen was significantly weaker than the expected average. The target load level of βf_c was not reached during the first displacement cycle. Nonetheless, all of the specimens exhibited a similar trend: a slowing of damage development with increasing cycle count [3]. The use of constant displacement amplitude, as a loading protocol, complicates the comparison of results with conventional fatigue testing based on constant stress amplitudes.

Post-loading examination

Figure 6a gives a post-loading, external view of the pervious concrete for the case of unroughened aggregates. Although small cracks are evident, structural integrity is maintained. A longitudinal section of one such specimen, illuminated by UV light, reveals extensive microcracking particularly along the aggregate-matrix interfaces (Fig. 6b). One objective is to correlate the development of these micro cracks with cycle count. Here, too, distribution of the matrix phase within the cross-section differs greatly from the idealized model shown in Fig. 1.

3 Computational modeling

As previously noted, spherical aggregates were selected to facilitate the computational modeling of the test specimens. By making a series of lateral cuts and imaging the cut sections, the sphere centers can be located using basic stereological principles.

Figure 7 shows one such reconstruction of a pervious concrete specimen. The numerical specimen is based on a Voronoi tessellation of a set of nodes, which serves to represent the pervious concrete as a three-phase composite. The aggregate, matrix, and aggregate-matrix interface phases are explicitly represented by lattice elements that interconnect the nodes, as described by Asahina et al. [4] for the case of model concrete. There is close correspondence between the physical and numerical specimens with respect to ag-

gregate positioning. However, inspection of Figs. 6, 7 and 8 reveals an important difference: the model assumes the matrix to be of uniform thickness over the aggregate surfaces, whereas the actual distribution of the matrix phase is highly nonuniform.

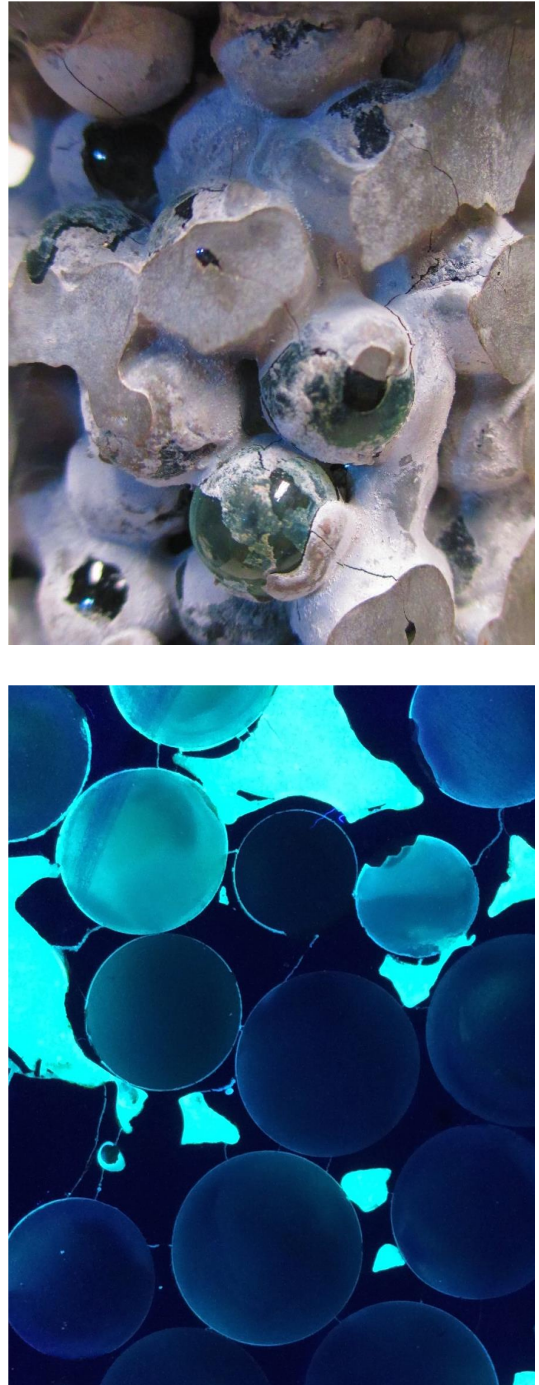


Figure 6: Microcracking along aggregate-matrix interface: a) external view; b) cross-section view

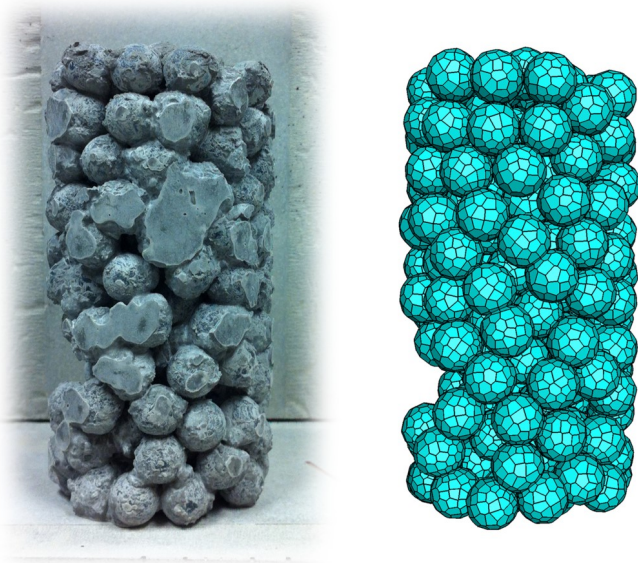


Figure 7: Physical and numerical specimens of porous concrete

Nonetheless, the three-phase modeling of the composite offers opportunities for simulating material breakdown under loading. Figure 9 illustrates the modeling of progressive debonding of a spherical inclusion within a solid matrix phase [4]. Behavior of the interface can be controlled in terms of the normal stress σ_n and shear stress τ , relative to the interface strength f_n . Whereas the fatigue resistance of pervious concrete is significantly more complicated, this form of lattice modeling is a rational means for simulating such behavior. Ongoing work involves realistic representations of the matrix distribution and cyclic load effects on the material bridges between aggregates.

4 Conclusions

As the range of applications of pervious concrete continues to grow, its resistance to cyclic loading is of increasing interest. This paper provides preliminary results from a combined experimental and computational study of this problem. The following conclusions can be made:

- As expected, fatigue resistance is af-

ected by the bond properties of the aggregate-matrix interface. Specimens made with (as-provided) glass spherical aggregates displayed extensive debonding along the aggregate-matrix interface. Roughening the aggregate surfaces reduced debonding and improved composite resistance to loading.

- Similar to observations of ordinary concrete, fatigue behavior of pervious concrete appears to be separated into different regimes: damage accumulates rapidly in the early loading cycles, followed by stable, progressive damage development prior to failure.

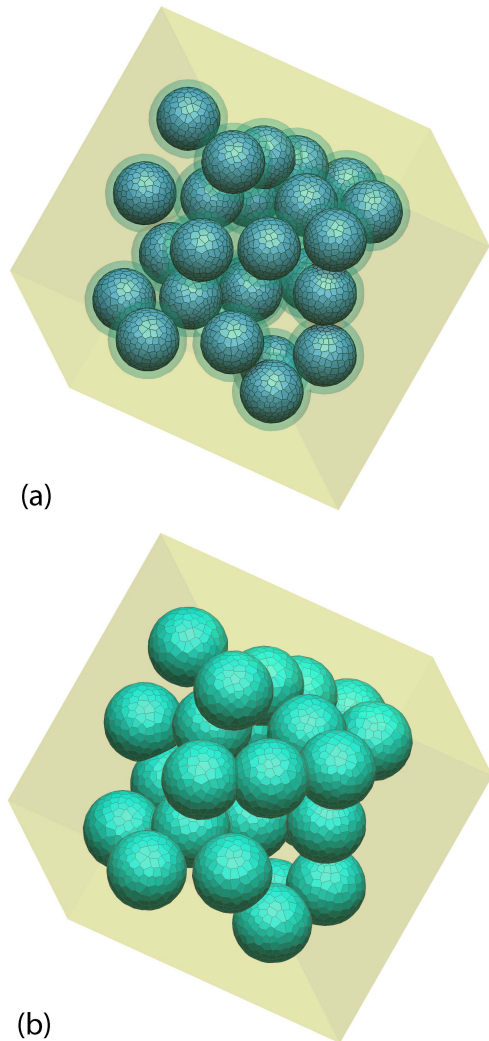


Figure 8: Discretization of a multiphase composite: a) spherical aggregates; and b) matrix coating of uniform thickness

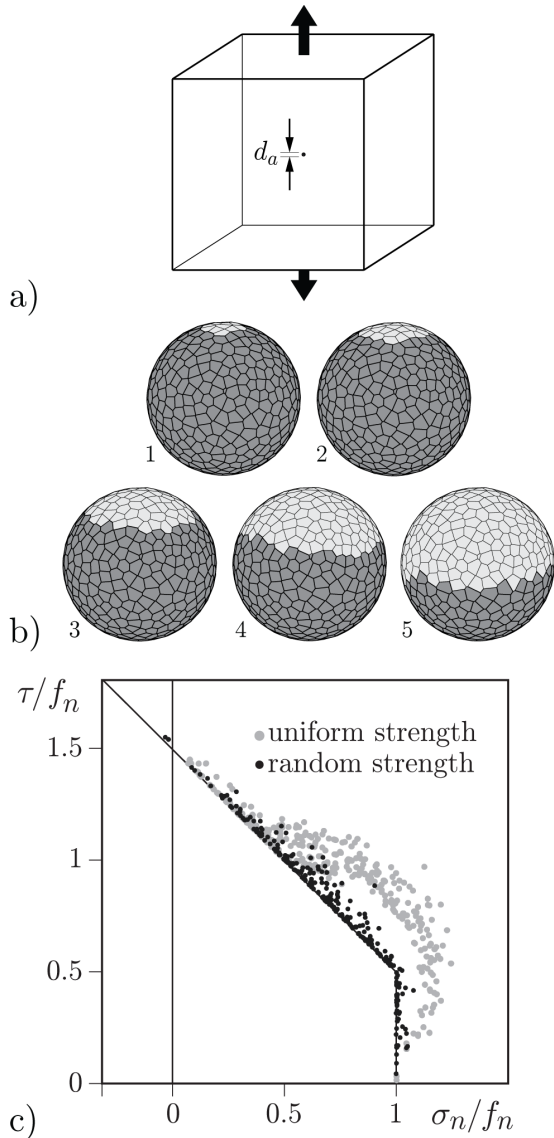


Figure 9: (a) Spherical inclusion within a vertical tension field; (b) stages of inclusion debonding; and (c) distribution of fracture events about the fracture surface (adapted from Asahina et al. [4])

- The value of these preliminary investigations is limited by the variability of the test specimens. Such variability stems from the presence of large irregular porosity and difficulties in producing nominally identical specimens at the small scale. Our current efforts are toward reducing this variability and improving the statistical significance of the test program.

- Lattice models are a potentially effective means for simulating pervious concrete as a multiphase material. Developmental needs include modeling the nonuniform distribution of the matrix phase and cyclic load effects on the material bridges between aggregates.

Acknowledgements

The authors appreciate the contributions of Dr. Kunhwi Kim at Lawrence Berkeley National Laboratory, who was primarily responsible for the multiphase discretizations presented in Figs. 7 and 8.

REFERENCES

- [1] Taranai, M., Mizuguchi, H., Hatanaka, S., Katahira, H., Nakazawa, T., Yanagibashi, K., Kunieda, M. 2003. Design, construction and recent applications of porous concrete in Japan. In *Proceedings of the 28th Conference on Our World in Concrete & Structures*; pp. 121-130.
- [2] Sumanasooriya, M.S., and Neithalath, N. 2011. Pore structure features of pervious concretes proportioned for desired porosities and their performance prediction. *Cement and Concrete Composites* **33**: 778-787. [doi:10.1016/j.cemconcomp.2011.06.002](https://doi.org/10.1016/j.cemconcomp.2011.06.002)
- [3] Maheshwari, A., Ichimaru, S., and Bolander, J.E. 2015. Characterization of fatigue properties of porous concrete. In *5th International Conference on Construction Materials (CONMAT 2015)* Whistler, BC, Canada (CD-ROM).
- [4] Asahina, D., Landis, E.N., and Bolander, J.E. (2011). Modeling of phase interfaces during pre-critical crack growth in concrete, *Cement and Concrete Composites* **33**(9): 966-977. [doi:10.1016/j.cemconcomp.2011.01.007](https://doi.org/10.1016/j.cemconcomp.2011.01.007)